



A combined study of quantum chemical calculation and molecular docking of some hydantoin and thiohydantoin related compounds

Mukta Das & M Abul Kashem Liton*

Department of Chemistry, Mawlana Bhashani Science and Technology University, Santosh, Tangail-1902, Bangladesh

*E-mail: akiltonchemmbstu@gmail.com

Received 20 July 2021; accepted (revised) 16 September 2022

The various classes of hydantoin and thiohydantoin compounds, many of which have extensive biological activities, have been intensively investigated in recent years. The quantum chemical properties and the molecular docking of a set of seven hydantoin and thiohydantoin related heterocyclic compounds containing cyclic urea and thiourea nuclei have been studied here. Dipole moment, frontier orbital gap, absolute hardness, and total energy of these compounds have been investigated. These compounds have been subsequently docked against the ligand-binding domain of the human androgen receptor (hAR). Molecular docking against the human androgen receptor demonstrates the variation in ligand binding affinity and show that TRP751, ARG752, GLU681, ASN756, and ALA748 amino acids play a critical role in ligand binding. According to molecular docking studies, L2 exhibits the best binding affinity of -8.3 kcal/mol with AR. Therefore, our studies suggest that the compound (L2) may be a promising candidate for further evaluation for PCa prevention or management.

Keywords: hAR, PCa, Molecular docking, Binding affinity, Frontier orbital gap

Since the discovery of imidazole in the 1840s, due to its extensive potential applications in medicinal chemistry as drugs, human-made materials, artificial acceptors, agrochemicals, biomimetic catalysts, supramolecular ligands, and so on, the development of imidazole-based research compounds has been very rapidly growing and increasingly active field¹⁻⁵. Hydantoins [imidazolidine-2,4-dione and 2-thioxo-imidazolidine-4-one] containing compounds show a wide variety of pharmacological and biological activities, including antimicrobial activity (antifungal, antibacterial)⁶⁻⁸, anti-diabetic⁹, antitumor¹⁰, anti-inflammatory¹⁰, anti-HIV¹¹, anticancer¹²⁻¹⁶, anti-hypertensive¹⁷ and anticonvulsant^{18,19} activities. In clinical use, several medicines, such as phenytoin, nitrofurantoin, and enzalutamide, have reinforced the importance of the hydantoin scaffold in drug discovery. There are five potential substituent sites for hydantoin, including two hydrogen bond acceptors and two hydrogen bond donors²⁰. Clinically approved drugs such as phenytoin (1), mephentoin (2), ethotoin (3), and fosphenytoin (4) as anticonvulsants; nitrofurantoin (5) and dantrium (6) as muscle relaxants; and nilutamide (7), and enzalutamide (8) as androgen receptor antagonists are representative pharmacological compounds²⁰ (Fig. 1). Androgen receptor AR antagonists is a soluble protein widely

used in clinical applications such as agonists for hypogonadism, whereas antagonists for prostate cancer therapy²¹. The second most common cancer diagnosis in males and the world's fifth leading cause of death is prostate cancer²². According to current cancer statistics, in the United States, the total number of identified new cases and deaths from PCa are 191,930 and 33,330, respectively²³. AR is a ligand-dependent transcription factor that belongs to the superfamily of nuclear receptors and plays a crucial role in the normal development of the prostate^{24,25}. It is understood that androgen hormones and their executor androgen receptors regulate crucial roles in PCa initiation and progression²⁶. Many drug-like molecules that bind to the AR, including substituted hydantoin and thiohydantoins, have recently been summarized by researchers²⁷⁻²⁹. Cyproterone acetate, flutamide, and bicalutamide are popular drugs that cause acute and long-term toxicity and develop drug resistance in patients³⁰.

In the present study, we used PyRx Auto Dock Vina software to perform molecular docking studies and assess all the compounds (L1-L7). Using AutoDock Vina software, the binding affinity of the widely used drugs for PCa viz., Bicalutamide, Darolutamide, Abiraterone, Nilutamide, and Enzalutamide was also assessed and then compared

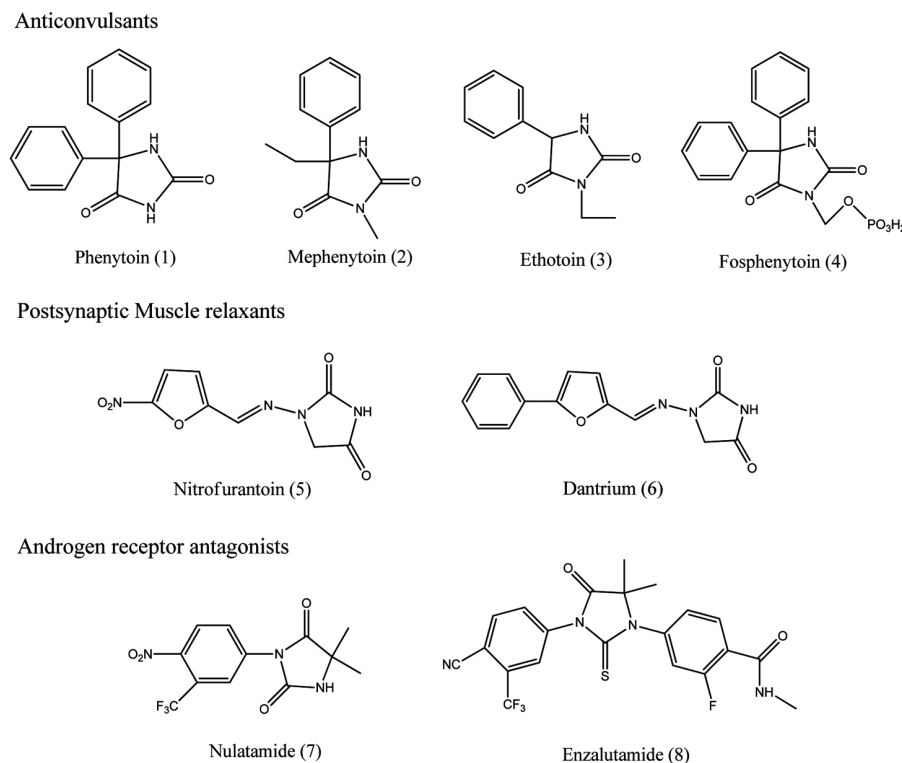


Fig. 1 — Structures of some commercially available hydantoin and thiohydantoin

with the binding affinity of the compounds (L1-L7) to find the active compounds that can function as anti-prostate cancer drugs³¹. Besides, quantum chemical descriptors of hydantoin and thiohydantoin compounds, including total energy, HOMO energy, LUMO energy, HOMO-LUMO energy gap, absolute hardness, and dipole moment in various solvents, were also being studied.

Experimental Section

General methods

In these experiments, all the chemicals and reagents were purchased from Sigma Aldrich and were used as pure. Following the literature procedure of Armarego and Chai³², purification and drying of reagents and solvents were carried out. On Merck aluminium sheets pre-coated with Kiessel gel, 60 GF254 of 0.25-mm thickness, thin layer chromatographic analysis was performed. All the melting points in an open glass capillary were calculated using the Stuart melting point apparatus (Model: SMP 10) and are uncorrected. Infrared spectra were acquired using KBr discs (4000–400 cm^{-1}) on a Perkin Elmer Spectrum-II FT-IR spectrometer.

Synthesis

By the literature procedure of Muccioli *et al.*³³, seven (7) compounds were prepared by direct heating instead of micro-wave assistance. All of the synthesized compounds shown in Table 1 were confirmed with melting point and IR spectrum analysis. Due to the prime emphasis on computational study, the synthetic section was not included in this manuscript.

Computational Methods

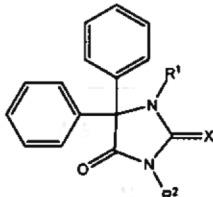
Quantum chemical calculation

Optimization of the structure, calculation of quantum chemical descriptors like total energy, HOMO-LUMO energy, absolute hardness, and dipole moment were carried out by MOPAC 2016 software³⁴ using the semi-empirical (PM6) method³⁵ in various solvents.

Ligands optimization, protein preparation, and molecular docking

Gauss View 6.0³⁶ was used to generate 3D structures of the synthesized compounds, and geometry optimization was carried out using Gaussian 09 software package³⁷ at semi-empirical PM6 method³⁵ in the vacuum phase. The three-dimensional

Table 1 — Synthesized compounds for computational study



5,5-Diphenyl-imidazolidine-2,4-dione moiety

Compound ID	R ¹	R ²	X
5,5-Diphenyl-2-thioxoimidazolidine-4-one (L1)	H	H	S
3,5,5-Triphenyl-2-thioxoimidazolidine-4-one (L2)	H	C ₆ H ₅ (phenyl)	S
3-Ethyl-5,5-diphenyl-2-thioxoimidazolidine-4-one (L3)	H	CH ₃ -CH ₂	S
1,3-Diethyl-5,5-diphenyl-2-thioxoimidazolidine-4-one (L4)	CH ₃ -CH ₂	CH ₃ -CH ₂	S
5,5-Diphenylimidazolidine-2,4-dione (L5)	H	H	O
3-Ethyl-5,5-Diphenylimidazolidine-2,4-dione (L6)	H	CH ₃ -CH ₂	O
3,5,5-Triphenylimidazolidine-2,4-dione (L7)	H	C ₆ H ₅ (phenyl)	O

crystal structure of Human AR (PDB ID: 2AMA)³⁸ was retrieved from Protein Data Bank (<http://www.rcsb.org/pdb/home/home.do>). Computed Atlas of Surface Topography of Proteins (CAST p) program was used to identify the three major catalytic sites of the receptor molecule 2AMA (<http://sts.bioe.uic.edu/castp/>). The crystal structure of the protein was then optimized and checked by the Swiss-PDB viewer software package (version 4.1.0) based on their lowest energy content³⁹. In the crystal structure of the protein, some significant factors, such as improper bond order, side chain geometry, and missing hydrogen, were observed. The PyMol (version 2.4.0) software package was used to remove all the heteroatoms, water molecules, and inhibitors present in the structure by DeLano, 2002⁴⁰. In the identification of novel small molecular scaffolds, molecular docking plays a significant role in drug development. A critical aspect of structure-based drug design is estimating the binding affinity of the ligand-receptor complex at the receptor-binding site. PyRx Auto Dock Vina Wizard performed molecular docking studies with the flexible ligand and the rigid receptor. The grid box in Autodock Vina was created by the protein's binding site where the center was X: 25.45, Y: 6.63, Z: 5.36, and the dimensions were X: 30.14, Y: 32.59, and Z: 26.44. Finally, using the

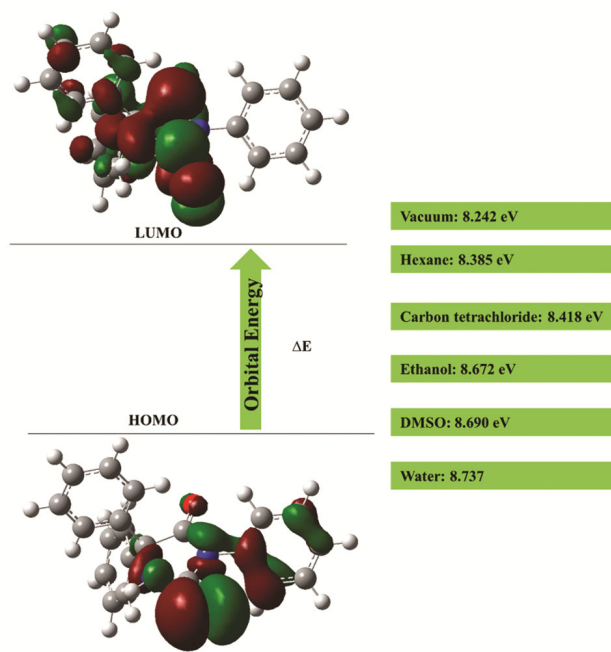


Fig. 2 — Frontier molecular orbitals of L2

AutoDock Vina software package, the binding affinity and nonbonding ligand-protein interactions were calculated³¹. In this method, binding affinities of the ligand-protein complex were calculated as negative scores in the kcal/mol unit. Here, stronger binding affinities suggest higher negative values. PyMol (version 2.4.0), BIOVIA Discovery Studio version 4.5, and ChimeraX-1.1⁴¹ were used to visualize and detect the noncovalent interaction in the docked ligand-protein complex.

Results and Discussion

Quantum chemical properties

In many properties of a compound, as well as in quantum chemistry, the highest occupied molecular orbitals (HOMO) and the lowest unoccupied molecular orbitals (LUMO), also known as frontier molecular orbitals (FMOs), play a significant role⁴². HOMO reflects the molecule's ability to donate an electron, and LUMO reflects the ability to accept an electron. Therefore, the charge transfer interactions in the molecule are shown by the HOMO-LUMO energy gap. The 3D structure of the frontier orbitals HOMO and LUMO of L2 is shown in Fig. 2.

The frontier orbital energy gap is a valuable parameter for understanding electrical properties, kinetic stability, optical polarizability, and chemical reactivity descriptors, such as hardness and softness, of a molecule. It's worth mentioning that a molecule

with a small frontier orbital gap is more polarizable and is commonly associated with a high chemical reactivity, poor kinetic stability and is often referred to as a soft molecule⁴³. On the other hand, a molecule with a large energy gap that is less polarizable is known as a hard molecule⁴⁴. Electrophilicity reflects energy reduction due to the maximum electron flow between HOMO (donor) and LUMO (acceptor). In the case of L2, the lower value of the frontier orbital gap indicates it is more reactive and less stable (Table 2).

Chemical hardness (η) was evaluated from the HOMO and LUMO energies using the following equation.⁴⁵

$$\eta = (\epsilon_{\text{LUMO}} - \epsilon_{\text{HOMO}})/2$$

Where, ϵ_{HOMO} and ϵ_{LUMO} are the energies of the HOMO and LUMO orbitals, respectively. Another significant electronic property is the dipole moment in a molecule that strongly depends on the charge transfer from one atom to another. It is mainly used to

Table 2 — Calculated quantum chemical properties of the synthesized compounds in different solvents

ID	Media	E_T	ϵ_{HOMO}	ϵ_{LUMO}	ΔE	μ	η
L1	Vacuum	-2823.88207	-9.091	-0.791	8.300	5.721	4.150
	Hexane	-2824.10333	-9.366	-0.888	8.478	6.624	4.239
	Carbon tetrachloride	-2824.14774	-9.433	-0.905	8.528	6.865	4.264
	Ethanol	-2824.54998	-9.902	-1.082	8.820	8.527	4.410
	DMSO	-2824.57388	-9.906	-1.088	8.818	8.661	4.409
	Water	-2824.59619	-9.908	-1.048	8.860	8.680	4.430
L2	Vacuum	-3612.20091	-8.964	-0.722	8.242	4.492	4.121
	Hexane	-3612.42040	-9.210	-0.825	8.385	5.487	4.193
	Carbon tetrachloride	-3612.47026	-9.267	-0.849	8.418	5.680	4.209
	Ethanol	-3612.87197	-9.747	-1.075	8.672	7.415	4.336
	DMSO	-3612.89577	-9.778	-1.088	8.690	7.498	4.345
	Water	-3612.95165	-9.816	-1.079	8.737	7.612	4.369
L3	Vacuum	-3123.46720	-8.937	-0.670	8.267	4.347	4.134
	Hexane	-3123.70059	-9.211	-0.763	8.448	5.453	4.224
	Carbon tetrachloride	-3123.73664	-9.291	-0.795	8.496	5.661	4.248
	Ethanol	-3124.15739	-9.759	-1.000	8.759	7.471	4.379
	DMSO	-3124.16016	-9.803	-1.018	8.785	7.667	4.392
	Water	-3124.19103	-9.817	-1.023	8.794	7.546	4.397
L4	Vacuum	-3423.01711	-8.778	-0.567	8.211	4.686	4.105
	Hexane	-3423.22988	-9.060	-0.690	8.370	5.716	4.185
	Carbon tetrachloride	-3423.27359	-9.128	-0.716	8.412	5.944	4.206
	Ethanol	-3423.62700	-9.667	-0.955	8.712	7.927	4.356
	DMSO	-3423.61647	-9.729	-0.957	8.772	8.171	4.386
	Water	-3423.67876	-9.717	-0.973	8.744	7.981	4.372
L5	Vacuum	-2941.40309	-9.862	-0.406	9.456	4.169	4.728
	Hexane	-2941.56071	-9.907	-0.367	9.540	4.469	4.77
	Carbon tetrachloride	-2941.62206	-9.895	-0.395	9.500	4.617	4.75
	Ethanol	-2941.89371	-9.939	-0.533	9.406	5.403	4.703
	DMSO	-2941.90470	-9.933	-0.526	9.407	5.425	4.703
	Water	-2941.92822	-9.954	-0.551	9.403	5.486	4.701
L6	Vacuum	-3240.98741	-9.742	-0.301	9.441	2.621	4.720
	Hexane	-3241.17206	-9.790	-0.328	9.462	3.051	4.731
	Carbon tetrachloride	-3241.20220	-9.807	-0.332	9.475	3.155	4.737
	Ethanol	-3241.50080	-9.863	-0.463	9.400	4.052	4.700
	DMSO	-3241.51981	-9.863	-0.480	9.383	4.157	4.691
	Water	-3241.53705	-9.892	-0.489	9.403	4.102	4.701
L7	Vacuum	-3729.79996	-9.150	-0.416	8.734	3.292	4.367
	Hexane	-3729.96757	-9.298	-0.457	8.841	3.693	4.421
	Carbon tetrachloride	-3729.99972	-9.324	-0.463	8.861	3.781	4.431
	Ethanol	-3730.28513	-9.586	-0.615	8.971	4.495	4.485
	DMSO	-3730.30481	-9.597	-0.633	8.964	4.572	4.482
	Water	-3730.33169	-9.620	-0.635	8.985	4.531	4.493

study the intermolecular interactions involving the Vander Waal type dipole-dipole forces, *etc.* since the greater the dipole moment, the stronger will be the intermolecular interactions⁴². The total energy (E_T), energy gap ($\Delta E = \epsilon_{LUMO} - \epsilon_{HOMO}$), and dipole moment (μ) have an effect on the stability of a molecule. To investigate the energetic behavior of the synthesized compounds, we have performed optimization in six different kinds of solvents, namely vacuum, water, ethanol, dimethyl sulfoxide (DMSO), hexane, and carbon tetrachloride. The calculated total energy, frontier orbital gap, dipole moment, and absolute hardness values for all the compounds are demonstrated in Table 2. Where E_T , ϵ_{HOMO} , ϵ_{LUMO} , ΔE , and η are represented in electron volt (eV) unit and μ , is represented in debye (D). The calculated results showed that the total energies of compounds in the solvent are lower than in the vacuum phase. HOMO-LUMO energy gap values indicate lower values in the vacuum phase than in the solvent phase for all compounds. As the solvent polarity increases, the values of the HOMO-LUMO energy gap increase. There is an exception to this solvent effect for L1 in DMSO, L4 in water, L5 in CCl_4 , EtOH, DMSO and water, L6 in EtOH, DMSO and water, and L7 in DMSO, whose energy gap is decreased in these solvents. The broadening of the HOMO-LUMO gap is mainly related to their HOMO levels, which are shifted to lower (that is, more negative) energies upon solvation. Increasing the HOMO-LUMO gap usually reflects high excitation energy and is associated with low chemical reactivity. Thus, except for L5 and L6, all compounds in the solvent are more stable than in the vacuum. By changing the media from vacuum to solvent, the dipole moments of the compound-solvent system increase. The calculated results showed that L1 in all solvents has the maximum total energy, most immense dipole moment value, and L5 and L6 have the maximum energy gap between frontier orbitals and maximum absolute hardness. Based on the energy gap, hardness and dipole moment of L2 in different media can be arranged as follow:

Water > DMSO > Ethanol > Carbon tetrachloride > Hexane > Vacuum

Molecular docking study

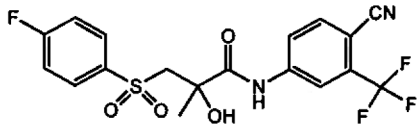
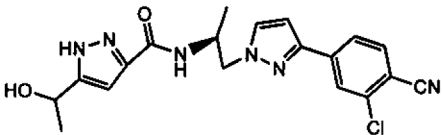
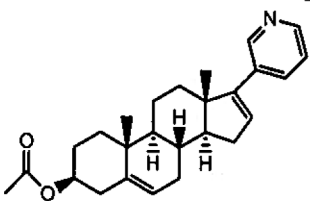
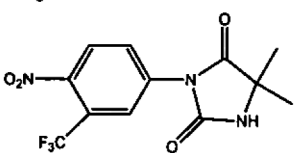
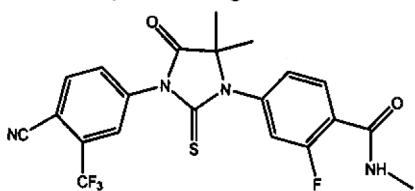
Molecular docking simulation between human androgen receptor 2AMA and hydantoin and thiohydantoin derivatives L1–L7 was performed using Autodock Vina. We identified the active pockets of 2AMA using CAST p during the initial part of the study to predict three catalytic sites in the receptor molecule with enormous volumes (Table 3)⁴⁶. The first pocket of the AR (PDB ID: 2AMA) has an area of 352.7 and a volume of 191.8, the second identified pocket has an area of 79.6 and a volume of 17.9, and the third active site has an area of 37.7 and a volume of 9.6. The best ligand-binding site was identified using these reported active sites. In the identified binding sites of human androgen receptor 2AMA, we then docked several commercially available PCa drugs to compare the binding energy of the synthesized compounds. In the study, commercially available PCa drugs were used as controls to decide the threshold values with respect to the binding affinity energies of controls. Our study expressed that Bicalutamide with the binding affinity of -9.7 kcal/mol followed by Darolutamide (-9.6 kcal/mol), Abiraterone (-8.7 kcal/mol), Nilutamide (-8.4 kcal/mol), and Enzalutamide (-8.1 kcal/mol) exhibited the best docking energy among the commercially available PCa drugs (Table 4).

The interactions of amino acids between hAR as the target and these compounds as ligands have also been identified, and detailed diagrams of ligand-receptor interaction are given in Fig. 3. Noncovalent interactions such as hydrogen bonds, hydrophobic interactions, and electrostatic interactions are found to be involved in the binding of ligands with 2AMA when the poses are predicted with AutoDock Vina. In this study; L1-L7 exhibited a binding affinity of -7.0 kcal/mol, -8.3 kcal/mol, -6.9 kcal/mol,

Table 3 — Identified active sites of receptor 2AMA with the corresponding interacting residues

S. No.	Area	Volume	Interacting residues
1	352.7	191.8	GLU681, PRO682, GLY683, VAL684, VAL685, LEU701, LEU704, ASN705, LEU707, GLY708, GLN711, HIS714, VAL715, TRP718, TRP741, MET742, LEU744, MET745, VAL746, ALA748, MET749, TRP751, ARG752, TYR763, PHE764, ALA765, PRO766, MET780, MET787, PHE804, LYS808, LEU873, PHE876, THR877, LEU880, PHE891, MET895
2	79.6	17.9	TYR739, SER740, MET742, GLY743, LEU744, LEU811, SER814, ILE815, GLN867, PRO868, ALA870, ARG871, HIS874, ILE906, GLY909, VAL911, LYS912, PRO913, TYR915
3	37.7	9.6	ARG786, HIS789, LEU790, GLU793, LEU862, SER865, ILE869

Table 4 — Binding affinity energies and the interacting catalytic sites of the commercially available PCa drugs

Commercially available drugs for PCa	Structure	Binding affinity (kcal/mol)	Interacting residues
Bicalutamide		-9.7	First pocket
Darolutamide		-9.6	First pocket
Abiraterone		-8.7	First pocket
Nilutamide		-8.4	First pocket
Enzalutamide		-8.1	First pocket

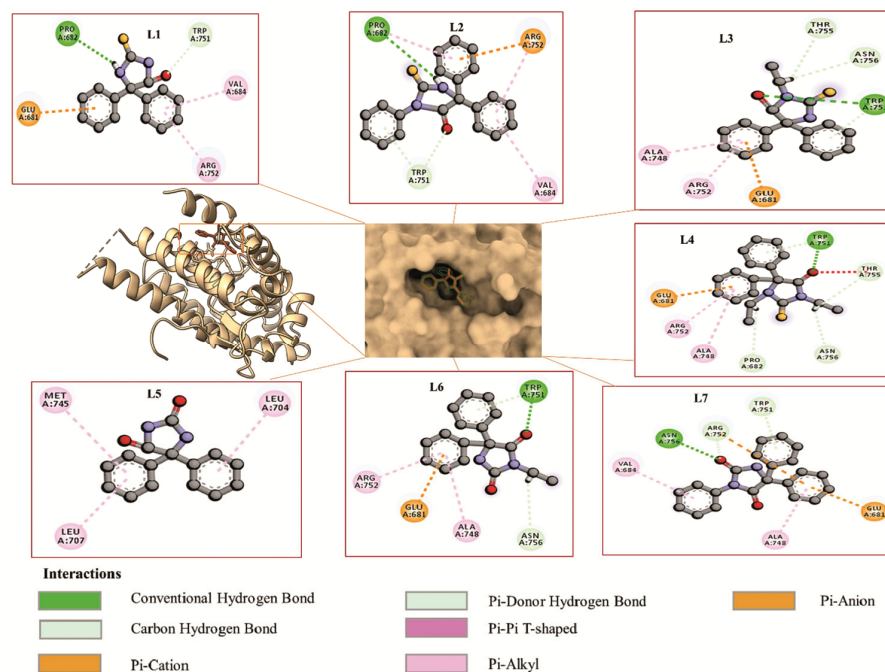
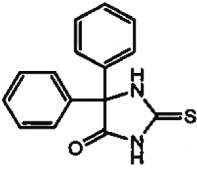
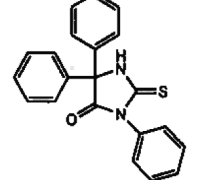
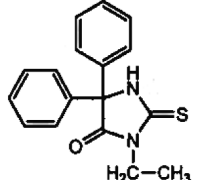
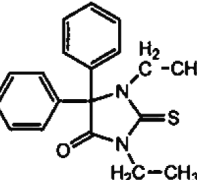
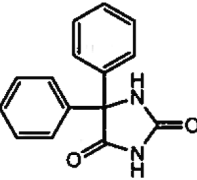
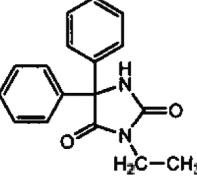
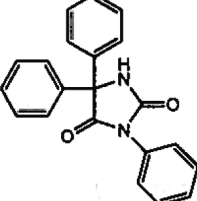


Fig. 3 — Nonbonding interactions of compounds (L1-L7) with 2AMA (Pose predicted by AutoDock Vina)

Table 5 — Docking results of compounds (L1-L7) with AR using AutoDock Vina

Entry	Chemical structure	Binding affinity energy (kcal/mol)
L1		-7.0
L2		-8.3
L3		-6.9
L4		-6.9
L5		-7.9
L6		-6.9
L7		-7.6

-6.9 kcal/mol, -7.9 kcal/mol, -6.9 kcal/mol, and -7.6 kcal/mol, respectively (Table 5).

In the L1-2AMA complex, the ligand is stabilized by two hydrogen bonds, one hydrophobic and two electrostatic interactions. Three hydrogen bonds, five hydrophobic bonds, and one electrostatic bond

stabilize the L2-2AMA complex. L3 is found to form five hydrogen bonds, four hydrophobic bonds, and one electrostatic bond with 2AMA, whereas six hydrogen bonds, four hydrophobic bonds, and one electrostatic bond are observed in the L4-2AMA complex. L5 has no hydrogen bond and electrostatic

Table 6 — Nonbonding interactions of compounds (L1-L7) with 2AMA (Pose predicted by AutoDock Vina)

Drug candidate	Hydrogen bond (AA...Ligand)	Hydrophobic interaction (AA...Ligand)	Electrostatic interaction (AA...Ligand)
L1	PRO682(2.267) C-O...H-N TRP751 (2.061) C-H...O-C	GLU681 (3.750) Pi-Anion	VAL684 (5.138) Pi-Alkyl ARG752 (4.234) Pi-Alkyl
L2	PRO682(2.498) C-O...H-N TRP751 (2.419) C-H...O-C TRP751 (2.622) Pi-Donor	TRP751 (4.543) Pi-Pi T-shaped TRP751 (5.751) Pi-Pi T-shaped VAL684 (4.649) Pi-Alkyl ARG752 (4.306) Pi-Alkyl PRO682 (5.042) Pi-Alkyl	ARG752 (3.800) Pi-Cation
L3	TRP751 (2.913) N-H...O-C TRP751(2.744) C-H...O-C TRP751 (2.579) Pi-Donor THR755(2.878) C-O...H-C ASN756 (2.827) C-O...H-C	TRP751 (4.478) Pi-Pi T-shaped TRP751 (5.666) Pi-Pi T-shaped ALA748 (4.882) Pi-Alkyl ARG752 (4.788) Pi-Alkyl	GLU681 (3.413) Pi-Anion
L4	TRP751 (2.897) N-H...O-C TRP751 (2.814) C-H...O-C TRP751 (2.544) Pi-Donor PRO682 (2.884) C-O...H-C THR755 (2.993) C-O...H-C ASN756 (2.862) C-O...H-C	TRP751 (4.445) Pi-Pi T-shaped TRP751 (5.619) Pi-Pi T-shaped ALA748 (4.877) Pi-Alkyl ARG752 (4.639) Pi-Alkyl	GLU681 (3.543) Pi-Anion
L5	-	LEU704 (5.499) Pi-Alkyl LEU707 (4.913) Pi-Alkyl MET745 (5.148) Pi-Alkyl	-
L6	TRP751 (2.879) N-H...O-C TRP751(2.745) C-H...O-C ASN756 (2.805) C-O...H-C TRP751 (2.582) Pi-Donor	TRP751 (4.473) Pi-Pi T-shaped TRP751 (5.666) Pi-Pi T-shaped ALA748 (4.893) Pi-Alkyl ARG752 (4.794) Pi-Alkyl	GLU681 (3.409) Pi-Anion
L7	ASN756 (2.150) N-H...O-C ARG752 (2.532) C-H...O-C TRP751 (2.629) Pi-Donor	TRP751 (4.520) Pi-Pi T-shaped ALA748 (4.592) Pi-Alkyl ARG752 (4.863) Pi-Alkyl VAL684 (5.311) Pi-Alkyl	ARG752 (4.212) Pi-Cation GLU681 (3.365) Pi-Anion

interactions with the protein but has three hydrophobic interactions. On the other hand, four hydrogen bonds, four hydrophobic bonds, and one electrostatic bond stabilize the L6-2AMA complex. The L7-2AMA complex is stabilized by three hydrogen bonds, four hydrophobic bonds, and two electrostatic bonds. The best ligand binding affinity was observed for L2. The details of the docking results of all the compounds are mentioned in Table 6.

Most of the compounds exhibited interactions with protein residues like TRP751, ARG752, GLU681, ASN756, and ALA748. Among all docked complexes, the amino acid TRP751 was commonly found in H-bonding interaction except L5. Interestingly, the amino acid TRP751 was also found in hydrophobic interaction with all the ligands except L1 and L5. The higher the binding energy is, the weaker the interaction is and *vice versa*. L5 and L7 had binding energy more than enzalutamide whereas,

L2 had lower binding energy values than the standard drug enzalutamide, emphasizing its high affinity for the androgen receptor than enzalutamide. The lowest binding energy was obtained for the compound L2 (−8.3 kcal/mol), while the highest energy result (−6.9 kcal/mol) was obtained for compounds L3, L4, and L6 in terms of binding energy. The results showed that the compound L2 had the highest affinity to bind with the androgen receptor. Besides, the formation of three hydrogen bonds in the compound L2 with PRO682 and TRP751 further contributed to the stability of the system, allowing the molecules to maintain a stable conformation in the active site. From the orbital picture of H bonding and interaction (Fig. 4), it was noticeable that the hydrogen bonding was shown with both donor and acceptor regions while the donor region was larger than the acceptor region. The oxygen atom reveals the part of the hydrogen acceptor, and the benzene ring contains the donor part.

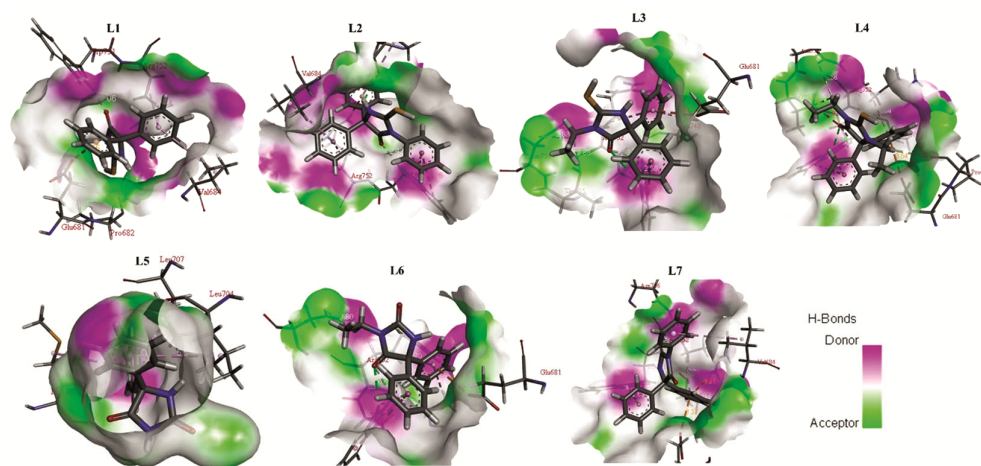


Fig. 4 — 3D H bonding between amino acid residue and compounds (L1-L7)

Conclusion

The quantum chemical study on all the compounds was carried out to find the total energy, frontier orbital energies, absolute hardness, and dipole moment, which indicates both chemical stability and chemical reactivity. Besides, the present quantum chemical study may play an essential role in understanding the dynamics of these molecules. HOMO-LUMO gap suggests L2 is the most reactive compound, which is clearly shown in the docking study. The focus of this paper is on molecular docking to determine the interactions between synthesized compounds and hAR. These compounds demonstrate a significant number of noncovalent interactions with the binding site residues of 2AMA, including hydrogen bond, hydrophobic interaction, and electrostatic interaction. Overall, we conclude that all the compounds have the required qualities to be effective anti-prostate cancer drugs against Human AR, where L2 shows better affinity than the standard drug enzalutamide. For the future synthesis of novel hydantoin and thiohydantoin analogues, these compounds may serve as a prominent scaffold that could function as promising androgen antagonists to treat prostate cancer. Therefore, it is worth to carry out further studies on them at both *in vitro* and *in vivo* levels to apply for PCa prevention and/ or management.

Supplementary Information

Spectral data, Frontier molecular orbitals of all the synthesized compounds, and the docking results with different poses of the synthesized compounds and commercially available PCa drugs with Androgen receptor (2AMA) are available in the website <http://nopr.nispr.res.in/handle/123456789/58776>.

Acknowledgements

The authors express their gratitude to the Department of Chemistry, Mawlana Bhashani Science and Technology University, Santosh, Tangail-1902.

Conflict of Interest

The authors declare no conflict of interest.

References

- 1 Forte B, Malgesini B, Piutti C, Quartieri F, Scolaro A & Papeo G, *Mar Drugs*, 7 (2009) 705.
- 2 Jin Z & Muscarine, *Nat Prod Rep*, 28 (2011) 1143.
- 3 Hill R A, *Annu Rep Prog Chem Sect*, 105 (2009) 150.
- 4 Jiang H Y, Zhou C H, Luo K, Chen H, Lan J B & Xie R G, *J Mol Catal Chem*, 260 (2006) 288.
- 5 Gao G, Xiao R, Yuan Y, Zhou C H, You J S & Xie R G, *J Chem Res*, 2002 (2002) 262.
- 6 Martan J, Enisz J, Hosztafi S & Timer T, *J Agri food Chem*, 41 (1993) 148.
- 7 Handzlik J, Szymanska E, Chevalier J, Otrebska E, Kiec-Kononowicz K, Pages J M & Alibert S, *Eur J Med Chem*, 46 (2011) 5807.
- 8 Fujisaki F, Shoji K, Shimodouzo M, Kashige N, Miake F & Sumoto K, *Chem Pharm Bull*, 58 (2010) 1123.
- 9 Sergent D, Wang Q, Sasaki N A & Ouazzani J, *Bioorg Med Chem Lett*, 18 (2008) 4332.
- 10 Ahmed K I, *Carbohydr Res*, 306 (1998) 567.
- 11 Comber R N, Reynolds R C, Friedeich J D, Magaikian R A, Buckheit R W, Truss J S, Shannon W M & Secrist J A, *J Med Chem*, 35 (1992) 3567.
- 12 Kavitha C V, Nambiar M, Kumar C S A, Choudhary B, Muniyappa K, Rangappa K S & Raghavan S C, *Biochem Pharmacol*, 77 (2009) 348.
- 13 Suzen S & Buyukbingol E, *Farmaco*, 55 (2000) 246.
- 14 Carmi C, Cavazzoni A, Zuliani V, Lodola A, Bordi F, Plazzi P V, Alfieri R R, Petronini P G & Mor M, *Bioorg Med Chem Lett*, 16 (2006) 4021.
- 15 Basappa C S, Kumar C S A, Swamy N, Sugahara K & Rangappa K S, *Bioorg Med Chem*, 17 (2009) 4928.
- 16 Jung M E, Ouk S, Yoo D, Sawyers C L, Chen C, Tran C & Wongvipat J, *J Med Chem*, 53 (2010) 2779.

- 17 Menendez J C, Diaz M P, Belleverl C & Sollhuber M M, *Eur J Med Chem*, 27 (1992) 66.
- 18 Zhu Q F, Pan Y H, Xu Z X, Li R M, Qiu G G, Xu W J, Ke X B, Wu L M & Hu X M, *Eur J Med Chem*, 44 (2009) 296.
- 19 Byrtus H, Obniska J, Czopek A & Nski K K, *Arch Pharm*, 344 (2011) 231.
- 20 Cho S, Kim S & Shin D, *Eur J Med Chem*, 164 (2019) 517.
- 21 Gao W, Bohl E C & Dalton T J, *Chem Rev*, 105 (2005) 3352.
- 22 Rawla P, *World J Oncol*, 10 (2019) 63.
- 23 Cancer Stat Facts: Prostate Cancer, National Cancer Institute, Surveillance, Epidemiology, & End Results Program <https://seer.cancer.gov/statfacts/html/prost.html>.
- 24 Brown C J, Goss S J, Lubahn D B, Joseph D R, Wilson E M, French F S & Wilard H F, *Am J Hum Genet*, 44 (1989) 264.
- 25 Mangelsdorf D J, Thummel C & Beato M, *Cell*, 83 (1995) 835.
- 26 Suzuki H, Ueda T, Ichikawa T & Ito H, *EndocrRelat Cancer*, 10 (2003) 209.
- 27 Nique F, Hebbe S, Peixoto C, Annoot D, Lefrançois M J, Duval E, Michoux L, Triballeau N, Lemoullec M J, Mollat P, Thauvin M, Prange T, Minet D, Lacroix C P, Jagerschmidt T, Fleury D, Guedin D & Deprez P, *J Med Chem*, 55 (2012) 8225.
- 28 Zhang X, Allan G F, Sbriscia T, Linton O, Lundeen S G & Sui Z, *Bioorg Med Chem Lett*, 16 (2006) 5763.
- 29 Zuo M, Xu X, Xie Z, Ge R, Zhang Z, Li Z, Bian & Jinlei, *Eur J Med Chem*, 125 (2017) 1002.
- 30 Singh A N, Baruah M M & Sharma N, *Cancer Scientific Reports*, 7 (2017) 1955.
- 31 Trott O & Olson A J, *J Comput Chem*, 31 (2010) 455.
- 32 Armarego W L F & Chai C L L, *Purification of Laboratory Chemicals*, 5th Edn (Butterworth Heinemann, London) (2003).
- 33 Muccioli G G, Poupaert J H, Woulers J, Norberg B, Poppitz W, Scriba G K E & Lambert D M, *Tetrahedron*, 59 (2003) 1301.
- 34 Stewart J J P, MOPAC2016 (Stewart Computational Chemistry, Colorado Springs, CO, USA), <http://OpenMOPAC.net> (2016).
- 35 Stewart J J P, *J Mol Model*, 13 (2007) 1173.
- 36 Roy D, Todd K, Millam A, & John M, Gauss View, Version 6, Semichem Inc.: Shawnee Mission, KS (2016).
- 37 Frisch M J, Trucks G W, Schlegel H B, Scuseria G E, Robb M A, Cheeseman J R, Scalmani G, Barone V, Mennucci B & Petersson G A, Gaussian 09, A.02 Wallingford CT: Gaussian, Inc. <https://doi.org/111> (2009).
- 38 Tran K P D J S, Lucco P T, Cantin L, Blanchet J, Labrie F & Breton R, *Protein Science*, 15 (2006) 987.
- 39 Guex N & Peitsch M C, *Electrophoresis*, 18 (1997) 2714.
- 40 DeLano W L, The PyMOL Molecular Graphics System. Delano Scientific, San Carlos (2002).
- 41 Goddard T D, Huang C C, Meng E C, Pettersen E F, Couch G S, Morris J H & Ferrin T E, <https://www.ncbi.nlm.nih.gov/pubmed/28710774> *Protein Sci*, 27 (2018) 14.
- 42 Prasad O, Sinha L, Misra N, Narayan V, Kumar N & Pathak J, *J Mol Struct Theo chem*, 940 (2010) 82.
- 43 Pearson R G, *Proc Natl Acad Sci*, 83 (1986) 8440.
- 44 Fleming I, *Frontier Orbitals and Organic Chemical Reactions* (John Wiley and Sons, New York) (1976).
- 45 Martins Jr J S S, Souza H D S, Oliveira R F D, Alves F S, Lima E O, Cordeiro L V, Trindade E O, Lira B F, Rocha G B, Filho P F D A & Filho J M B, *J Braz Chem Soc*, 00 (2020) 1.
- 46 Dundas J, Ouyang Z, Tseng J, Binkowski A, Turpaz Y & Liang J, *Nucleic Acids Res*, 34 (2006) W116.